

# ChemComm

Accepted Manuscript



This is an *Accepted Manuscript*, which has been through the Royal Society of Chemistry peer review process and has been accepted for publication.

*Accepted Manuscripts* are published online shortly after acceptance, before technical editing, formatting and proof reading. Using this free service, authors can make their results available to the community, in citable form, before we publish the edited article. We will replace this *Accepted Manuscript* with the edited and formatted *Advance Article* as soon as it is available.

You can find more information about *Accepted Manuscripts* in the [Information for Authors](#).

Please note that technical editing may introduce minor changes to the text and/or graphics, which may alter content. The journal's standard [Terms & Conditions](#) and the [Ethical guidelines](#) still apply. In no event shall the Royal Society of Chemistry be held responsible for any errors or omissions in this *Accepted Manuscript* or any consequences arising from the use of any information it contains.



Journal Name

COMMUNICATION

## Facile synthesis of $\text{CuCo}_2\text{S}_4$ as a novel electrode material for ultrahigh supercapacitor performance

Received 00th January 2015,  
Accepted 00th January 2015

Jianhua Tang, Yuancai Ge, Jianfeng Shen\*, Mingxin Ye\*

DOI: 10.1039/x0xx00000x

www.rsc.org/

**$\text{CuCo}_2\text{S}_4$  nanoparticles demonstrating outstanding electrochemical performances were firstly synthesized through a simple solvothermal approach without using any templates.  $\text{CuCo}_2\text{S}_4$  synthesized in glycerol ( $\text{CuCo}_2\text{S}_4$ -Glycerol) fulfills an ultrahigh capacitance of  $5030 \text{ F g}^{-1}$  at  $20 \text{ A g}^{-1}$  in polysulfide electrolyte.**

In the wake of depletion of traditional energy resources and environmental pollution, supercapacitors (SCs) have attracted extensive attention for their various applications, such as portable electronics, hybrid electric vehicles, mobile communications, back-up power supplies, military devices, and large industrial equipment.<sup>[1]</sup> SCs have high specific power density, fast charge and discharge rates, and long cycle life, while the energy density is much lower than that of batteries.<sup>[2]</sup> To meet the demands for high capacitance storage applications, many research efforts have been focused on improving the specific capacitance of SCs electrode materials. Since the high power density of SCs is one of the most important requirements, it is unwise to achieve "high specific capacitance" through testing the electrode materials at a low rate.<sup>[3]</sup> Therefore, the key challenge for current SCs in practical applications is to improve their specific capacitance at the high rate where SCs devices are required.<sup>[4]</sup> To this end, electrodes with large capacitance need to be developed and evaluated at the required high rate.

In recent years, due to the excellent electroactive abilities, metal sulfides have been widely proposed for the SCs.<sup>[5]</sup> In particular, ternary sulfides have attracted much attention, due to their excellent properties in the potential applications for energy storage.<sup>[6]</sup> Compared to the single-component sulfides, ternary sulfides can combine the contributions from both metal ions and offer richer redox reactions.<sup>[7]</sup> Therefore, it is significant to exploit ternary sulfides used for SCs. Some

research works about ternary sulfides used for SCs have been explored and exhibited excellent capacitive performance.<sup>[2b, 7, 8]</sup> Their values of capacitances can be found in the table S1 (ESI). It can be clearly seen that the previously reported ternary sulfides obtained high capacitance at relatively low current density. In addition, current researches based on the ternary sulfides mainly focused on the nickel cobalt sulfides. Partial substitution of Co or Ni with low-cost and benign elements in the spinel structure could reduce the cost. To the best of our knowledge, up to now, no report is available on  $\text{CuCo}_2\text{S}_4$ -based electrode materials for SCs. In this work, our aim is to prepare ultrahigh performance SC electrode materials based on  $\text{CuCo}_2\text{S}_4$  and achieve high capacitance at the required high current density.

$\text{CuCo}_2\text{S}_4$  nanoparticles were synthesized through a simple solvothermal route using different solvents (deionized water, glycol and glycerol). The detailed preparation procedure can be found in the ESI. The electrochemical behaviours of the as-prepared samples as novel electrode materials for SCs were investigated using cyclic voltammograms (CV), galvanostatic charge/discharge (GCD) and electrochemical impedance spectroscopy (EIS) on an electrochemistry workstation (Autolab PGSTAT128N). Compared to the previously reported ternary sulfides, the as-prepared  $\text{CuCo}_2\text{S}_4$  exhibited higher specific capacitances at the high current density in polysulfide electrolyte.<sup>[6, 9]</sup>

The crystallographic structures of  $\text{CuCo}_2\text{S}_4$  synthesized in different solvents were analysed by X-ray powder diffraction (XRD). All diffraction patterns reveal the successful formation of the carrollite structure phase of  $\text{CuCo}_2\text{S}_4$  (according to the JCPDS card No. 42-1450), as shown in Fig. 1a. The main diffraction peaks appear at  $26.6^\circ$ ,  $31.3^\circ$ ,  $38.0^\circ$ ,  $47.0^\circ$ ,  $50.0^\circ$  and  $54.8^\circ$  respectively correspond to the (0 2 2), (1 1 3), (0 0 4), (2 2 4), (1 1 5) and (0 4 4) planes of the carrollite phase of  $\text{CuCo}_2\text{S}_4$  structure.  $\text{CuCo}_2\text{S}_4$  synthesized in different solvents show different degrees of crystallization. Among the samples,  $\text{CuCo}_2\text{S}_4$ -Water presents the highest degree of crystallization, while that of  $\text{CuCo}_2\text{S}_4$ -Glycerol is the lowest which can be explained by considering the viscosity of the solvents. The low

<sup>a</sup> Institute of Special Materials and Technology, Fudan University, Shanghai, 200433, China

E-mail address: mxye@fudan.edu.cn (Mingxin Ye), jfshen@fudan.edu.cn (Jianfeng Shen)

† Electronic Supplementary Information (ESI) available: [Experimental section, Equ.S1–S3, Fig. S1–S4, and Table. S1]. See DOI: 10.1039/x0xx00000x

viscosity of water leads to the high diffusion rate of ions, which is benefit to the crystalline growth. In contrast, in glycerol, the slow diffusion rates of ions resulting from the high viscosity, can greatly suppress crystalline growth.<sup>[10]</sup>

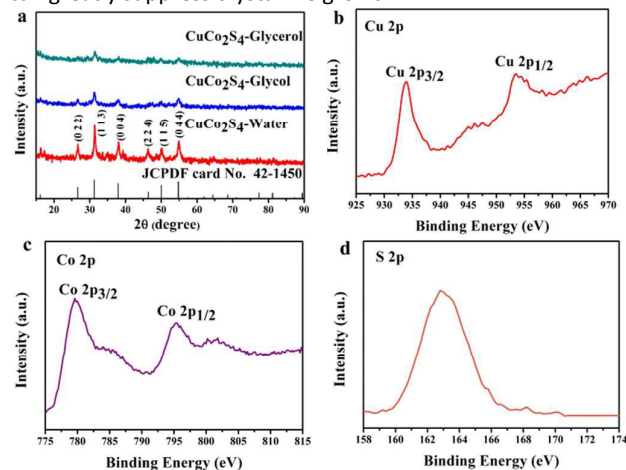


Fig. 1 XRD patterns (a) of  $\text{CuCo}_2\text{S}_4$ -Water,  $\text{CuCo}_2\text{S}_4$ -Glycol and  $\text{CuCo}_2\text{S}_4$ -Glycerol; XPS curves of  $\text{CuCo}_2\text{S}_4$ -Glycerol Cu 2p (b), Co 2p (c) and S 2p (d).

The XRD peaks of spinel sulfides composed of different elements are very close. In order to prove that the as-prepared samples contained qualitative elements, X-ray photoelectron spectroscopy (XPS) characterization was further performed to evaluate the chemical bonding state of the  $\text{CuCo}_2\text{S}_4$ -Glycerol. The Cu 2p spectrum (Fig. 1b) presented two major  $2p_{3/2}$  (933.8 eV) and  $2p_{1/2}$  (953.4 eV) spin-orbit peaks and the Cu  $2p_{3/2}$  curve region was assigned to  $\text{Cu}^+$ ,  $\text{Cu}^{2+}$  and  $\text{Cu}^{3+}$ .<sup>[11]</sup> As shown in Fig. 1c, two prominent peaks at binding energies of 779.6 and 795.2 eV corresponded to the Co  $2p_{3/2}$  and Co  $2p_{1/2}$  spin-orbit peaks, respectively, which confirmed the existence of two kinds of cobalt oxidation state:  $\text{Co}^{2+}$  and  $\text{Co}^{3+}$ .<sup>[12]</sup> The binding energy of the S 2p peaks is 162.8 eV, indicating that the S species exist as  $\text{S}^{2-}$ .<sup>[13]</sup> Thus, the successful formation of  $\text{CuCo}_2\text{S}_4$  can be confirmed through the XRD and XPS characterizations.

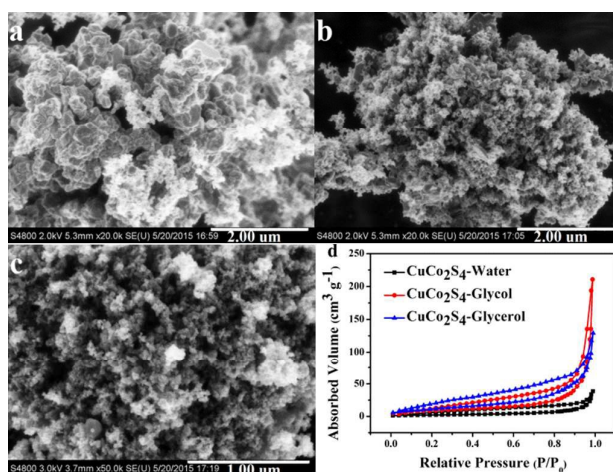


Fig. 2 SEM images of  $\text{CuCo}_2\text{S}_4$ -Water (a),  $\text{CuCo}_2\text{S}_4$ -Glycol (b) and  $\text{CuCo}_2\text{S}_4$ -Glycerol (c); Nitrogen adsorption/desorption isotherms (d) of  $\text{CuCo}_2\text{S}_4$ -Water,  $\text{CuCo}_2\text{S}_4$ -Glycol and  $\text{CuCo}_2\text{S}_4$ -Glycerol.

The morphology of the as-prepared samples was investigated by the scanning electron microscopy (SEM) technique. As shown in Fig. 2a-c, the as-prepared  $\text{CuCo}_2\text{S}_4$  samples in different solvents show similar morphologies comprising of numerous irregular nanoparticles. Among the samples, the agglomeration of  $\text{CuCo}_2\text{S}_4$ -Water is more obvious than that of the other two samples. In order to investigate surface property of the as-prepared  $\text{CuCo}_2\text{S}_4$  samples, nitrogen adsorption-desorption were measured. As determined by nitrogen sorption measurements (Fig. 2d), the specific surface areas of the  $\text{CuCo}_2\text{S}_4$ -Water,  $\text{CuCo}_2\text{S}_4$ -Glycol and  $\text{CuCo}_2\text{S}_4$ -Glycerol are 8.046, 32.591, and 43.843  $\text{m}^2 \text{g}^{-1}$ , respectively. Owing to the agglomeration, the specific surface area of the  $\text{CuCo}_2\text{S}_4$ -Water is much smaller than those of  $\text{CuCo}_2\text{S}_4$ -Glycol and  $\text{CuCo}_2\text{S}_4$ -Glycerol. Fig. S1 shows the pore size distribution of  $\text{CuCo}_2\text{S}_4$ -Water,  $\text{CuCo}_2\text{S}_4$ -Glycol and  $\text{CuCo}_2\text{S}_4$ -Glycerol obtained from the desorption branch of the isotherm. The average pore sizes of  $\text{CuCo}_2\text{S}_4$ -Water,  $\text{CuCo}_2\text{S}_4$ -Glycol and  $\text{CuCo}_2\text{S}_4$ -Glycerol were 29.68, 40.02, and 18.23 nm, respectively. The high BET specific surface area and the mesoporous structure can offer more diffusion paths for the electrolyte transport and increase reactive sites between electrode and electrolyte, which can greatly improve the electrochemical performance of  $\text{CuCo}_2\text{S}_4$ .<sup>[14]</sup> To further obtain the details of morphology, TEM images of  $\text{CuCo}_2\text{S}_4$ -Glycerol (Fig. 3 and Fig. S2) were taken. It is clearly demonstrated that the sample is mainly composed of lots of irregular nanoparticles with the size less than 100 nm, which is consistent with SEM results. Furthermore, the measured fringe lattice spacing of 0.28 nm corresponds to the (1 1 3) interplanar distance of  $\text{CuCo}_2\text{S}_4$  (Fig. 3b).

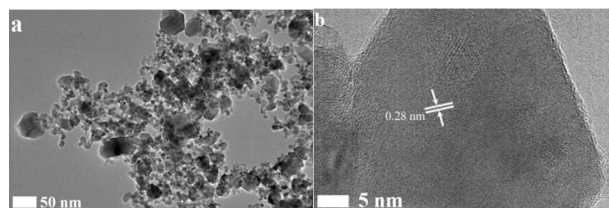


Fig. 3 TEM images of  $\text{CuCo}_2\text{S}_4$ -Glycerol.

To evaluate potential applications in SCs, the electrodes were fabricated using  $\text{CuCo}_2\text{S}_4$  applied on Ni foam. The loading mass of the active materials on Ni foam current collector was around 5 mg, and each working electrode had a geometric surface area of  $1 \text{ cm}^2$ . Electrochemical tests were conducted in a three-electrode configuration using polysulfide electrolyte. Fig. 4a presents the CV curves of the  $\text{CuCo}_2\text{S}_4$ -Water,  $\text{CuCo}_2\text{S}_4$ -Glycol and  $\text{CuCo}_2\text{S}_4$ -Glycerol at a scan rate of  $5 \text{ mV s}^{-1}$  in a potential window of  $-0.25$  to  $0.4 \text{ V}$  vs  $\text{Ag}/\text{AgCl}$ . The shapes of the CV curves of  $\text{CuCo}_2\text{S}_4$  are clearly different from the ideal rectangular shapes related to the electric double-layer

capacitance. This demonstrates that the as-prepared  $\text{CuCo}_2\text{S}_4$  samples are excellent promising capacitive materials with pseudocapacitance. Obviously, the pairs of redox reaction peaks not only correspond to the reversible faradaic processes of  $\text{Co}^{4+}/\text{Co}^{3+}$  and  $\text{Cu}^{2+}/\text{Cu}^+$ , but also may be owing to the redox reaction of polysulfide at the electrode electrolyte interface.<sup>[15]</sup> So far, there have been some previously reported works about the electrochemistry of polysulfide solvents.<sup>[16]</sup> However, owing to the complicated reactions involved in the polysulfide electrolyte, its exact chemical mechanisms are presently not well understood. The possible redox reaction process is discussed in the Eqn. (1)-(3) (ESI). The CV measurements of  $\text{CuCo}_2\text{S}_4$ -Water,  $\text{CuCo}_2\text{S}_4$ -Glycol and  $\text{CuCo}_2\text{S}_4$ -Glycerol were also carried out at different scan rates ranging from 5 to 100  $\text{mV s}^{-1}$  (Fig. S3). According to the eqn. (4) (ESI), the specific capacitances of  $\text{CuCo}_2\text{S}_4$ -Water,  $\text{CuCo}_2\text{S}_4$ -Glycol and  $\text{CuCo}_2\text{S}_4$ -Glycerol electrodes obtained at 5  $\text{mV s}^{-1}$  are 2737, 3647 and 5148  $\text{F g}^{-1}$ , respectively.

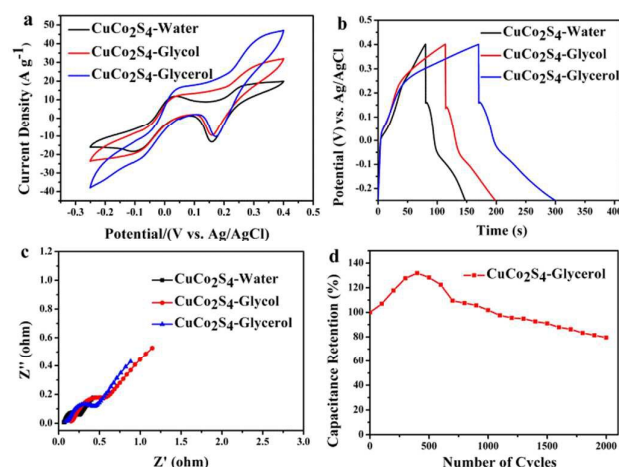


Fig. 4 CV curves at 5  $\text{mV s}^{-1}$  (a), GCD curves at 20  $\text{A g}^{-1}$  (b) and EIS plots (c) of  $\text{CuCo}_2\text{S}_4$ -Water,  $\text{CuCo}_2\text{S}_4$ -Glycol and  $\text{CuCo}_2\text{S}_4$ -Glycerol; cycling performances of  $\text{CuCo}_2\text{S}_4$ -Glycerol electrode at 70  $\text{A g}^{-1}$  for 2000 cycles (d).

To further investigate the electrochemical performances of  $\text{CuCo}_2\text{S}_4$  electrodes, galvanostatic charge/discharge measurements were conducted at various current densities with an electrochemical window of -0.25 to 0.4 V vs Ag/AgCl. Fig. 4b shows the charge-discharge behaviors of  $\text{CuCo}_2\text{S}_4$ -Water,  $\text{CuCo}_2\text{S}_4$ -Glycol and  $\text{CuCo}_2\text{S}_4$ -Glycerol electrodes at a current density of 20  $\text{A g}^{-1}$ . The charge-discharge curves of  $\text{CuCo}_2\text{S}_4$  show some curvature, which is due to redox transitions and corresponds to the typical redox couples in the CV curves. The specific capacitance values of  $\text{CuCo}_2\text{S}_4$ -Water,  $\text{CuCo}_2\text{S}_4$ -Glycol and  $\text{CuCo}_2\text{S}_4$ -Glycerol calculated from the charge-discharge tests are 2602, 3304 and 5030  $\text{F g}^{-1}$  at the current density of 20  $\text{A g}^{-1}$  by the Eqn. (5) (ESI). The high capacitance of  $\text{CuCo}_2\text{S}_4$  could be credited to the synergy effect between  $\text{CuCo}_2\text{S}_4$  and polysulfide electrolyte.<sup>[15]</sup> As shown in Fig. S4, the  $\text{CuCo}_2\text{S}_4$ -Glycerol electrode also fulfilled a relatively high specific capacitance of 1365  $\text{F g}^{-1}$  even at a very large

current density of 70  $\text{A g}^{-1}$ , which indicated excellent rate performance. The decreasing tendency of the capacitance of the samples demonstrates that parts of the electrode fail to react completely at a high current density. In the process of high-rate charge-discharge, the ionic motion in the electrolyte is controlled by diffusion owing to the time constraint, and the inside active material makes no contribution to charge storage.<sup>[17]</sup>

According to the cyclic voltammograms (CV), galvanostatic charge/discharge (GCD) measurements, the specific capacitance of the low crystalline  $\text{CuCo}_2\text{S}_4$ -Glycerol is evidently higher than those of the high crystalline  $\text{CuCo}_2\text{S}_4$ -Water and  $\text{CuCo}_2\text{S}_4$ -Glycol. The same results were also observed for low crystalline  $\text{Ni}(\text{OH})_2$  and  $\text{NiWO}_4$  which have higher capacitance than their high crystalline counterparts.<sup>[17, 18]</sup> Furthermore, the  $\text{CuCo}_2\text{S}_4$ -Glycol who obtains the highest capacitance possesses the biggest specific surface area among the three samples of  $\text{CuCo}_2\text{S}_4$ , while the capacitance of  $\text{CuCo}_2\text{S}_4$ -Water is much smaller than those of  $\text{CuCo}_2\text{S}_4$ -Glycol and  $\text{CuCo}_2\text{S}_4$ -Glycerol owing to the serious agglomeration and small specific surface area.

As a powerful measurement for researching the electrochemical behaviours of the  $\text{CuCo}_2\text{S}_4$  electrodes, EIS were also performed to investigate the charge transfer resistances. As shown in Fig. 4c, the impedance plots include a high frequency component (a partial semicircle) and a low-frequency component (an inclined line along the imaginary axis). As it can be seen, the values of equivalent series resistance (ESR) for  $\text{CuCo}_2\text{S}_4$ -Water,  $\text{CuCo}_2\text{S}_4$ -Glycol and  $\text{CuCo}_2\text{S}_4$ -Glycerol are 0.063, 0.150 and 0.088  $\Omega$ , respectively, indicating small bulk resistance of the  $\text{CuCo}_2\text{S}_4$  electrodes. The partial semicircle is attributable to the interfacial charge transfer resistance (Rct) at the electrode-electrolyte interface, which is mainly associated with the faradic reactions.<sup>[14]</sup> Rct for the  $\text{CuCo}_2\text{S}_4$ -Water,  $\text{CuCo}_2\text{S}_4$ -Glycol and  $\text{CuCo}_2\text{S}_4$ -Glycerol electrodes is 0.196, 0.437 and 0.361  $\Omega$ , respectively. In the effects of composite factors such as morphology, conductivity and electrode fabrication, the Rct of  $\text{CuCo}_2\text{S}_4$ -Water is lowest. The small Rct of the  $\text{CuCo}_2\text{S}_4$  electrodes demonstrates fast ion diffusion and electron transport. At the low frequency range, the inclined line called as Warburg impedance ( $W_s$ ) is related to electrolyte ions diffusion/transport through the host materials.<sup>[19]</sup> The relatively vertical lines in the low frequency region suggests that the ion diffusion in the electrolyte solution and the ions adsorption onto the electrode surface occur swiftly, which is an indication of capacitive behaviour of the  $\text{CuCo}_2\text{S}_4$  electrode materials. The small ESR, Rct and  $W_s$  of the  $\text{CuCo}_2\text{S}_4$  electrodes play an important role in improving the performance of SCs.

The long-term electrochemical stability of the electrode is one of the key parameters for the practical application of SCs.<sup>[8b]</sup> Therefore, the cycling stability of the  $\text{CuCo}_2\text{S}_4$ -Glycerol electrode was conducted at a current density of 70  $\text{A/g}^{-1}$  for 2000 cycles (Fig. 4d). For the electrode with  $\text{CuCo}_2\text{S}_4$ -Glycerol coating, the capacitance decreased 20.5% after 2000 cycles. The cycling stability is highly related to the structural stability of the electrodes. The specific capacitance of the  $\text{CuCo}_2\text{S}_4$ -

Glycerol electrode increased in the initial cycles, which was attributed to an activation process.<sup>[20]</sup>

The table S1 (ESI) summarizes some previous reports on the electrochemical performance of ternary sulfides. In comparison of these values, the CuCo<sub>2</sub>S<sub>4</sub> electrode materials can possess high values of specific capacitance at much higher current densities. What's more, in table S2 (ESI), the as-prepared CuCo<sub>2</sub>S<sub>4</sub> also show higher capacitance than the other sulfides in the same polysulfide electrolyte.

In conclusion, a simple solvothermal method was firstly used to synthesize CuCo<sub>2</sub>S<sub>4</sub> nanoparticles, and electrochemical measurements suggest their applications as novel electrode materials for ultrahigh capacitance SCs. The material CuCo<sub>2</sub>S<sub>4</sub>-Glycerol displays an ultrahigh capacitance of 5030 F g<sup>-1</sup> at 20 A g<sup>-1</sup> and even exhibits a high capacitance of 1365 F g<sup>-1</sup> at an extremely high current density of 70 A g<sup>-1</sup>. Compared to the previously reported ternary sulfides, the outstanding electrochemical properties of the CuCo<sub>2</sub>S<sub>4</sub> may result in potential applications for SCs.

#### ACKNOWLEDGMENT

This work was supported by National Natural Science Foundation of China (51202034).

#### Notes and references:

- 1 D. Yu, Q. Qian, L. Wei, W. Jiang, K. Goh, J. Wei, J. Zhang, Y. Chen, *Chem. Soc. Rev.* 2015, 44, 647-662.
- 2 (a) Y. Yang, G. Ruan, C. Xiang, G. Wang, J. M. Tour, *J. Am. Chem. Soc.* 2014, 136, 6187-6190; (b) L. Shen, J. Wang, G. Xu, H. Li, H. Dou, X. Zhang, *Adv. Energy. Mater.* 2015, 5, DOI: 10.1002/aenm.201400977.
- 3 T. H. Murray, *Science*. 2014, 343, 1208-1210.
- 4 D. Yu, K. Goh, H. Wang, L. Wei, W. Jiang, Q. Zhang, L. Dai, Y. Chen, *Nat. Nanotechnol.* 2014, 9, 555-562.
- 5 (a) Y. Li, K. Ye, K. Cheng, J. Yin, D. Cao, G. Wang, *J Power Sources*. 2015, 274, 943-950; (b) J. Wang, D. Chao, J. Liu, L. Li, L. Lai, J. Lin, Z. Shen, *Nano Energy*. 2014, 7, 151-160; (c) J. Rodríguez-Moreno, E. Navarrete-Astorga, E. A. Dalchiele, R. Schrebler, J. R. Ramos-Barrado, F. Martín, *Chem Commun*. 2014, 50, 5652; (d) Q. Zhang, C. Xu, B. Lu, *Electrochim Acta*. 2014, 132, 180-185.
- 6 J. Yang, Y. Zhang, C. Sun, G. Guo, W. Sun, W. Huang, Q. Yan, X. Dong, *J. Mater. Chem. A*. 2015, 3, 11462-11470.
- 7 S. Peng, L. Li, C. Li, H. Tan, R. Cai, H. Yu, S. Mhaisalkar, M. Srinivasan, S. Ramakrishna, Q. Yan, *Chem Commun*. 2013, 49, 10178.
- 8 (a) L. Mei, T. Yang, C. Xu, M. Zhang, L. Chen, Q. Li, T. Wang, *Nano Energy*. 2014, 3, 36-45; (b) J. Xiao, L. Wan, S. Yang, F. Xiao, S. Wang, *Nano Lett.* 2014, 14, 831-838.
- 9 (a) J. M. Chen, Z. Li, X. W. D. Lou, *Angew. Chem. Int. Edit.* 2015, 54, 10521-10524; (b) F. Luo, J. Li, H. Yuan, D. Xiao, *Electrochim Acta*. 2014, 123, 183-189; (c) Y. Tang, T. Chen, S. Yu, Y. Qiao, S. Mu, S. Zhang, Y. Zhao, L. Hou, W. Huang, F. Gao, *J Power Sources*. 2015, 295, 314-322; (d) H. Wan, J. Jiang, Y. Ruan, J. Yu, L. Zhang, H. Chen, L. Miao, S. Bie, *Part. Part. Syst. Char.* 2014, 31, 857-862.
- 10 H. Peng, G. Ma, J. Mu, K. Sun, Z. Lei, *Mater Lett.* 2014, 122, 25-28.
- 11 J. Cheng, H. Yan, Y. Lu, K. Qiu, X. Hou, J. Xu, L. Han, X. Liu, J. Kim, Y. Luo, *J. Mater. Chem. A*. 2015, 3, 9769-9776.
- 12 S. K. Bikkarolla, P. Papakonstantinou, *J Power Sources*. 2015, 281, 243-251.
- 13 X. Wang, B. Batter, Y. Xie, K. Pan, Y. Liao, C. Lv, M. Li, S. Sui, H. Fu, *J. Mater. Chem. A*. 2015, 3, 15905-15912.
- 14 Q. Wang, J. Yan, Y. Wang, T. Wei, M. Zhang, X. Jing, Z. Fan, *Carbon*. 2014, 67, 119-127.
- 15 L. Qian, X. Tian, L. Yang, J. Mao, H. Yuan, D. Xiao, *Rsc. Adv.* 2013, 3, 1703-1708.
- 16 (a) H. K. Jun, M. A. Careem, A. K. Arof, *Int. J. Photoenergy*. 2013, 2013, 1-10; (b) Z. Yang, C. Chen, C. Liu, H. Chang, *Chem Commun*. 2010, 46, 5485-5487; (c) N. S. A. Manan, L. Aldous, Y. Alias, P. Murray, L. J. Yellowlees, M. C. Lagunas, C. Hardacre, *J. Phys. Chem. B*. 2011, 115, 13873-13879.
- 17 H. B. Li, M. H. Yu, F. X. Wang, P. Liu, Y. Liang, J. Xiao, C. X. Wang, Y. X. Tong, G. W. Yang, *Nat Commun*. 2013, 4, 1894.
- 18 L. Niu, Z. Li, Y. Xu, J. Sun, W. Hong, X. Liu, J. Wang, S. Yang, *ACS. Appl. Mater. Inter.* 2013, 5, 8044-8052.
- 19 Y. X. Zhang, M. Huang, F. Li, X. L. Wang, Z. Q. Wen, *J Power Sources*. 2014, 246, 449-456.
- 20 A. Pendashteh, M. S. Rahmanifar, R. B. Kaner, M. F. Mousavi, *Chem Commun*. 2014, 50, 1972-1975.